Catalysis Letters, Vol. 114, Nos. 3–4, April 2007 (© 2007)
DOI: 10.1007/s10562-007-9054-4

A comparative study of gas phase esterification on solid acid catalysts

Kaewta Suwannakarn, Edgar Lotero, and James G. Goodwin Jr.*

Department of Chemical and Biomolecular Engineering, Clemson University, Clemson, SC 29634, USA

Received 22 November 2006; accepted 16 January 2007

For the first time, a comprehensive comparison of the intrinsic activities of solid acid catalysts in terms of turnover frequency (TOF) is reported for the gas-phase esterification of acetic acid with methanol. The catalysts studied included a zeolite (Hβ), two modified zirconias (sulfated zirconia, SZ; and tungstated zirconia, WZ), and an acidic resin-silica composite (Nafion/silica, SAC-13). Activities on a per weight basis decreased in the following order: H$\beta \sim$ SAC-13 $\gg$ SZ $>$ WZ at 130 °C. However, on a rate-per-site basis (TOF), all catalysts showed comparable activities. The TOF results suggest that the acid sites of these catalysts have similar capacity for effectively catalyzing esterification. All catalysts deactivated to a quasi-steady-state rate with TOS. Regeneration experiments suggested that catalyst deactivation was due mainly to site blockage by carbonaceous deposits. Selective poisoning experiments showed that the reaction predominately took place on Brønsted acid sites.

KEY WORDS: esterification in the gas-phase; acetic acid; Methanol; Hβ zeolite; sulfated zirconia; tungstated zirconia; Nafion/silica composite; SAC-13.

1. Introduction

Carboxylic acid esters constitute major components of numerous natural products and synthetic compounds. They are widely used as softeners, emulsifiers, dispersants, detergents, surfactants, and biodiesel fuel. In general, esters are prepared by the esterification of carboxylic acids with alcohols. The most common methodology for this reaction involves the utilization of liquid mineral acid catalysts such as sulfuric acid in batch reactors [1]. Current liquid-phase esterification processes pose several drawbacks such as equipment corrosion, difficulty in handling, and separation of products from the catalyst. For these reasons, the use of solid acid catalysts, which are non-corrosive, reusable, and can be easily separated from the reaction mixture, should provide an efficient and cost effective way to carry out acid-catalyzed esterification.

Many heterogeneous catalysts have been reported to be active in esterification: ion exchange resins [2,3], zeolites [4], supported metal oxides [5–7], supported heteropolyacids (HPAs) [8,9], and others [10–12]. Although studies of esterification over solid acid catalysts are numerous, most solid-catalyzed studies have used high temperature and pressure to enhance the performance of solid catalysts and to keep the reactants, especially low molecular weight alcohols, in the liquid-phase. Esterification is thermodynamically favored in the vapor phase due to higher values of the equilibrium constants in comparison with those for the liquid-phase reaction [13,14]. Moreover gas-phase esterification can be suitably conducted at 1:1 alcohol-to-acid molar ratios contrary to the common practice in liquid systems to employ excess alcohol to drive the reaction to completion. The use of excess alcohol in the starting mixture not only leads to higher energy consumption because of separation requirements, but may also have a negative effect on the catalyst activity [4,13].

In this work, different solid acid catalysts were studied for the gas-phase esterification reaction of equimolar ratios of acetic acid and methanol, including Nafion–SiO_2 composite (SAC-13), zeolite β (Hβ), sulfated zirconia (SZ), and tungstated zirconia (WZ) (representatives of acidic ion-exchange resin, zeolite, and metal oxide catalysts, respectively). Their catalytic activities were compared in terms of apparent activation energies, turnover frequencies, and deactivation-regeneration behavior. Although, a number of studies have been reported on the activity of solid catalysts for esterification reactions, to the best of our knowledge, no work has so far compared the performance of different solid acid catalysts for this reaction in terms of turnover frequency (TOF), i.e., intrinsic activity per measured site. Here for the first time, using catalyst activities and acid site concentrations, TOFs have been calculated in an attempt to compare the activity of different solid acid catalysts for gas-phase esterification in a way that more accurately represents their true catalytic ability.

2. Experimental

2.1. Materials

The protonated form of zeolite β (Hβ) was purchased from Zeolyst. Nafion/SiO_2 nanocomposite was obtained

*To whom correspondence should be addressed.
E-mail: james.goodwin@ces.clemson.edu

Table 1
Pretreatment methods and catalyst characterization results of the solid acids studied

Catalyst	Pretreatment method	Elemental analysis wt% (element)[f]	BET surface area[g] (m^2/g)	Average pore size diameter (nm)	Pore volume (cm^3/g)[h]	Surface acid site concentration (μmol/g)	XRD pattern
SAC-13	Dried at 100 °C for 2 h	0.4% (S)	418	>10[a]	>0.6[a]	131[b]	–
SZ	Calcined at 600 °C for 2 h	1.7% (S)	155	4.1	0.15	105 ± 12[c]	Tetragonal ZrO_2
WZ	Calcined at 700 °C for 2 h	13.7% (W)	115	5.1	0.15	59 ± 4[c]	Tetragonal ZrO_2
Hβ (Si:Al = 103[e])	Calcined at 500 °C for 2 h	42.7% (Si), 0.4% (Al)	620[a]	0.5 × 0.5 and 0.8 × 0.6[d]	0.35	130[b]	–

[a] Information provided by the supplier.
[b] Calculated from elemental analysis: sulfur content for SAC-13 and aluminum content for Hβ.
[c] Determined from NH_3 TPD.
[d] Zeolite pore dimensions.
[e] Calculated from elemental analysis.
[f] Maximum error = ±4%.
[g] Maximum error = ±4%.
[h] Maximum error = ±3%.

from Sigma-Aldrich. Sulfated zirconia and tungstated zirconia were kindly supplied by Magnesium Electron Inc. (MEI). All catalysts were crushed and/or sieved to 170/140 mesh particle size. Catalyst characteristics are summarized in table 1.

Acetic acid and methanol with > 99% purity, as reported by the supplier, were purchased from Sigma-Aldrich, and Acros, respectively.

2.2. Catalyst characterization

2.2.1. Elemental analysis and X-ray diffraction

Powder X-ray diffraction spectra were collected in the 5–90° 2P range for SZ, WZ, and zeolite Hβ with a Scintag XDS 2000 diffractometer using Cu K_α radiation with a wavelength of λ = 1.54 Å. Chemical analyses of the materials were carried out by Galbraith Laboratories.

2.2.2. BET analysis

The surface areas of the solid acids were determined by N_2 BET analysis (N_2, UHP, National Specialty Gases). The catalysts were degassed at 200 °C under vacuum for 3 h to desorb adsorbed molecules (mainly water) from the catalyst surface before BET measurements.

The pore volume and pore size distributions of SZ and WZ were calculated from the adsorption/desorption branches of the isotherms using the Barrett–Joyner–Halenda (BJH) method [15].

2.2.3. Temperature-programmed desorption of ammonia

Three hundred mg of SZ or WZ was heated up to 315 °C under 30 cc/min of He (UHP, National Specialty Gases) for 1 h to remove adsorbed volatile materials. Next, the sample was cooled down to room temperature and saturated in a 100 cc/min stream of 10% NH_3/He (Anhydrous grade, National Specialty Gases) for 2 h. The system was then purged at 60 °C for 4 h with 30 cc/min of He to eliminate physisorbed NH_3. For TPD, the temperature was ramped from 60 to 600 °C at a rate of 10 °C /min. A thermal conductivity detector was used to measure the NH_3 desorption profiles. For comparison purposes, 300 mg of SZ or WZ was pretreated under the same conditions but without NH_3 adsorption and the temperature ramped from 60 to 600 °C. This was used as a baseline to calculate acid site concentrations from NH_3 TPD data.

2.3. Esterification

Reaction was carried out in a differential fixed bed reactor (ID = 0.7 cm) at 100–140 °C and atmospheric pressure. Prior to reaction, SAC-13 was dehydrated under a flow of 30 cc/min of He (UHP, National Specialty Gases) at 100 °C for 2 h. The inorganic catalysts were pretreated *in situ* at 315 °C for 2 h under 30 cc/min of air (UHP zero grade air, National Specialty Gases) and then cooled down to 100 °C before the temperature was adjusted to the desired value under flowing He.

Gaseous acetic acid (HAc) and methanol (MeOH) were obtained from temperature controlled liquid saturators by passing through them known flow rates of He. The reactants were further mixed with additional He to vary concentrations and flow independently. Small amounts of catalysts were used to maintain differential conversion (< 10%) conditions: 20 mg for WZ or SZ, and 5 mg for SAC-13 or Hβ. In order to obtain a catalyst bed height/diameter greater than 1.5, an inert solid, α-Al_2O_3 (surface area = 3 m^2/g), was well mixed with the catalysts. α-Al_2O_3 showed insignificant activity for esterification as measured by blank experiments carried

out in the absence of a catalyst. The reactants (acetic acid and methanol) were introduced to the reactor in equimolar ratios with a total flow rate of 120 cc/min [P_{HAc} = 0.0085 atm, P_{MeOH} = 0.0085 atm]. Heating and insulating tapes were wrapped around the stainless-steel tubing of the reaction system to maintain a 120 °C temperature in order to avoid reagent condensation. Esterification can be autocatalyzed by acetic acid itself at moderate temperatures [16]; however, only a trace of methyl acetate was detected in the absence of a catalyst under these reaction conditions. The concentrations of the reactants at the reactor entrance and the effluent products were analyzed by a Varian CP-3380 gas chromatograph equipped with an FID detector and a fused silica column (60 m × 0.53 mm × 0.1 μL, coated with CP WAX 52 CB). Helium was the carrier gas.

3. Results and discussion

3.1. Catalyst characterization

Table 1 shows the surface areas, surface acidities, and XRD patterns determined for the catalysts employed in this study. The XRD results indicate that the pretreated zirconia-based oxides contained only the tetragonal phase of zirconia with the tungsten oxide or sulfate species existing only as amorphous species or small crystallites ≤5 nm in diameter. The diffraction pattern of Hβ was compared to literature powder X-ray diffraction data, confirming the correct structure and level of crystallinity.

The concentration of acid sites for zeolite Hβ was estimated from its Al content, assuming that every tetrahedral aluminum atom in the framework accounted for an acid site and that all these sites were accessible. Camiloti *et al.* [17] employed TPD of ammonia to determine the acidity of zeolite Hβ and found the NH_3/Al ratios were equal to one, suggesting that every aluminum atom provides an accessible potential site. Nevertheless, using an estimation of acid site density from the Al content should be considered to provide a maximum value for the concentration of active surface sites, meaning that TOFs calculated correspond to minimum TOF values. The number of acid sites for SAC-13 was estimated from its sulfur content since each sulfonic group constitutes an active site and all such groups in SAC-13 have been reported to be accessible for reaction [18].

The acid site concentrations of SZ and WZ measured by NH_3 TPD are in agreement with those previously reported by Kim *et al.* [19] (1.7 wt% S content) and Shimizu *et al.* [20] (16.6 wt% W content), respectively.

3.2. Reaction studies

Because of the relatively high boiling points of the reactants (64.7 °C for MeOH and 118 °C for HAc at 1 atm) and the presence of micro- and mesopores in most of the catalysts studied, pore condensation may take place and should be avoided in order to make a reasonable assessment of intrinsic catalyst activities. According to the Kelvin equation [21], 130 °C is the lowest temperature at which reaction can be carried out on Hβ without having capillary condensation of reagents (under our reaction conditions), assuming cylindrical shaped pores. For the mesoporous catalysts SZ and WZ, the threshold temperature for condensation is 100 °C. Due to the macroporous structure of SAC-13, pore condensation should occur below 90 °C. The onset of pore condensation was verified experimentally using reaction data, e.g., significant change in slope of Arrhenius plots (not shown). Reaction at appropriate temperatures (≥130 °C for Hβ, ≥100°C for SZ, WZ, and SAC-13) showed no pore condensation effects. Data is not reported nor used in determination of the apparent activation energies below the respective pore condensation temperatures of the various catalysts. For all catalysts, a reaction temperature of 130 °C was employed for comparison of TOF results.

The potential effect of internal and external mass transfer limitations was determined at a reaction temperature of 130 °C for Hβ (the most active, and most microporous catalyst). By varying the catalyst particle sizes in the range 89–297 μm, a change in the overall rate of reaction was not observed. Thus, intraparticle diffusional resistance of reactants did not affect our experimental results. By varying the total flow rate (100–150 cc/min), the rate of methyl acetate formation was insignificantly changed, suggesting that no external mass transfer effects were present. Hence, all further experiments were conducted with catalyst particle sizes 89–104 μm at the flow conditions of 120 cc/min.

Given the exothermic nature of esterification with ΔH_{rxn} = −19.1 kJ/mol (calculated using Aspen®), heat transfer limitations could also lead to kinetic data misinterpretation. Thus, all experiments were performed at low acetic acid conversions (below 10%) in a differential fixed bed reactor. An Arrhenius plot of the rate data versus 1/T (not shown) does not indicate any evidence for mass or heat transfer limitations. Apparent activation energies calculated (table 2) are in line with reaction controlling kinetics. All E_a values were in the range, 55–65 kJ/mol, with Hβ < SZ < SAC-13 < WZ. Note, the E_a value observed for SAC-13 is consistent with that previously reported by Liu *et al.* [18] of 51 kJ/mol for the liquid-phase esterification of acetic acid with methanol catalyzed by SAC-13. The dissimilarity in values (10 kJ/mol difference) may be explained by the low- and high-temperature regimes employed in these two studies. Initial rates reported in terms of TOF were employed in the Arrhenius plots to compare catalytic activities. As suggested by E_a values, all catalysts showed similar capacity to catalyze esterification efficiently, as confirmed by calculations of TOF values (discussed later).

Table 2
The apparent activation energies for gas-phase esterification of acetic acid with methanol on SAC-13, SZ, WZ, and Hβ

Catalysts	Apparent activation energy (kJ/mol)	Temperature range (°C)
SAC-13	61 ± 2	100–140
SZ	57 ± 1	100–140
WZ	65 ± 5	100–140
Hβ	55 ± 4	130–140

Figure 1 shows the evolution of esterification with time-on-stream (TOS) for the different solid catalysts reported as rate of formation of methyl acetate per gram of catalyst. All catalysts exhibited 100% selectivity for methyl acetate. The activity of Hβ was similar to that of SAC-13, followed by SZ and WZ in that order. The observed catalyst deactivation may be attributed to two possible factors: accumulation of water around the acid sites on the surface, and the deposit of carbonaceous materials.

Water is known to deactivate sulfuric acid used as the catalyst in the liquid-phase esterification of acetic acid with methanol by forming a strong hydration sphere around the protons [16]. Similar water induced deactivation appears to occur for solid acid Brønsted sites in SAC-13 [18]. Hence, water cluster formation around Brønsted sites in heterogeneous catalysts in general can be expected to cause deactivation. Under gas flow reaction conditions, there should be a more limited impact of water since it cannot build up large concentrations neither on the catalyst surface nor in the gas phase. Moreover, catalyst deactivation by water should be affected by surface hydrophobicity. For instance, Palani and Pandurangan [22] studied the effect of Si/Al ratios of Al-MCM-41catalysts used for the gas-phase esterification of acetic acid with amyl alcohol and found that higher acid conversions were obtained as the Si/Al ratio increased due to the capacity of the materials to expel water from the pores (greater hydrophobicity).

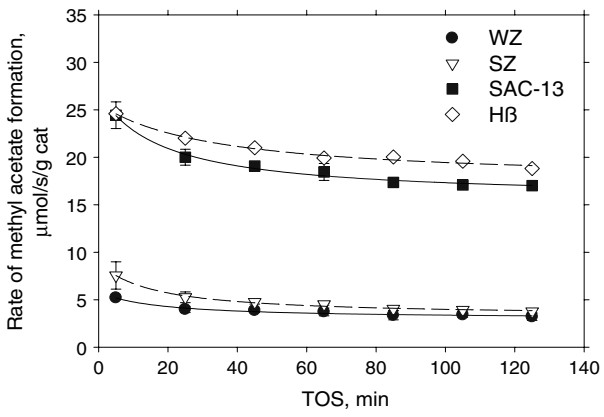

Figure 1. TOS catalyst activity for the gas-phase esterification of acetic acid with methanol at 130 °C, atmospheric pressure, molar ratio of methanol:acetic acid = 1.

However, since acid site concentrations in aluminosilicates decrease as the Si/Al ratio increases, there must be optimal catalyst composition that allows the achievement of maximum catalyst performance. In a different study, Mbaraka and Shanks [12] reported that further functionalization of mesoporous organosulfonic silicas with hydrophobic organic groups improved catalytic performance in the esterification of fatty acids with low molecular weight alcohols. Thus, as suggested from the reaction profiles in figure 1, under our experimental conditions, any deactivation by water accumulation on the catalyst surface seems to affect the catalyst activity of Hβ the least (Hβ, SAC-13, WZ, and SZ exhibited 23%, 30%, 35%, and 50% activity loss after 2 h TOS, respectively) due to its more hydrophobic surface, in line with what is expected.

For SZ, in principle, water produced as a byproduct can hydrolyze sulfate groups to H_2SO_4; however, under our experimental conditions (gas-phase reaction at lower that 10% conversion), one would not expect sulfur leaching by hydrolysis of sulfate groups, as substantiated by the almost complete recovery of activity upon re-calcination (section 3.4).

3.3. Comparison of initial reaction rate on a site basis (TOF)

Table 3 presents TOF values calculated using initial reaction rates at 5 min TOS (130 °C) and the concentration of acid sites reported in table 1. On a site basis, the order of activity was: zeolite Hβ ~ SAC-13 > WZ ~ SZ. Note that although Hβ and SAC-13 showed much higher activities (factor of four) per gram of catalyst than SZ and WZ, their activities were within a factor of two on a rate-per-site basis. Thus, the relative high catalytic activities of Hβ and SAC-13 in a per-weight basis can be attributed mostly to their higher acid site concentrations. Other factors, such as uncertainties in the estimation of "active" acid site concentrations (especially for WZ and SZ), different susceptibility to catalyst deactivation (given variations in surface hydrophobicity) and differences in acid site strengths, could have contributed to the observed TOF differences for esterification with the various catalysts. Based on all the potential sources of error, one is led to conclude that catalytic performance in terms of TOF for the series of

Table 3
Calculated initial TOF for gas-phase esterification of acetic acid with methanol at 130 °C

Catalyst	Initial rate (μmol/g cat/s)	TOF[a] (10^{-2} s^{-1})
Hβ	24.6 ± 0.1	18.9
SZ	7.5 ± 1.4	7.2
WZ	5.2 ± 0.2	8.9
SAC-13	24.4 ± 1.4	18.6

[a] Calculated based on acid site concentrations in table 1.

catalysts used in this study is very similar. This observation together with the fact that all catalysts yielded similar E_a values for esterification suggest that these materials are probably using sites with similar characteristics to carry out the reactions.

3.4. Deactivation and regeneration

The stability and the potential cause of catalyst deactivation were explored only for the inorganic catalysts due to the thermal instability of SAC-13 (decomposes at 250 °C). To examine catalyst regeneration, the inorganic catalysts (WZ, SZ, and Hβ) were re-calcined under a flow of air at 315 °C for 2 h. After re-calcination, the reaction profile produced by all inorganic catalysts resembled with some minor differences those obtained using the fresh catalysts (figure 2). It is noted that for SZ, even though the fresh and used catalysts gave rise to parallel reaction profiles, the total activity of the used catalyst was below that of the fresh catalyst. This indicates that a small population of active sites may have been irreversibly lost during deactivation or regeneration.

WZ regeneration was also examined by drying the used catalysts under a flow of He at 315 °C. This procedure was applied to eliminate mostly adsorbed moisture on the catalyst surface leaving behind carbonaceous deposits that could have been formed during the first reaction cycle. Formation of carbonaceous deposits can block active sites on WZ as other authors have reported. Bilbao-Elorriaga *et al.* [23] previously reported, for instance, catalyst deactivation due to "coke" deposition in gas- phase esterification of acetic acid and *n*-butanol for a SiO_2–Al_2O_3 catalyst. As can be seen in figure 3, after drying at 315 °C, WZ showed activity very close to that observed for the steady state activity of the fresh catalyst, suggesting that water accumulation have a minimal impact on catalyst deactivation and that formation of carbonaceous deposits is the major reason for catalyst deactivation on WZ.

Since water does not seem to be affecting the activity of WZ, we decided to probe the effect of water on this catalyst by pretreating a fresh sample of WZ with water vapor at the reaction temperature. As shown in figure 4, water pretreatment surprisingly increased the initial reaction rate, while steady state reaction rates were comparable for both fresh and water-pretreated catalysts. The unexpected enhancement of reaction rate at short TOS for water-pretreated WZ should be a consequence of the generation of Brønsted acid sites on this catalyst produced by water adsorption on Lewis acid sites. It is known that Lewis and Brønsted sites are easily exchangeable by adsorption-desorption of water molecules [24]. The observation of enhanced reaction rates with increased water concentrations has been reported previously for gas-phase esterification with a molybdate zirconia catalyst [24]. In that report, the authors also attributed the enhanced observed rate to a reversible formation of Brønsted sites by water adsorption on Mo oxide species on the catalyst surface. Hence, for the water-pretreated WZ catalyst, it is probably the reversible character of the water-formed sites that leads to reaction rate enhancement only at the initial stages of reaction.

3.5. Brønsted versus Lewis acidity

To further elucidate the role of Brønsted versus Lewis acid sites in esterification, poisoning experiments using

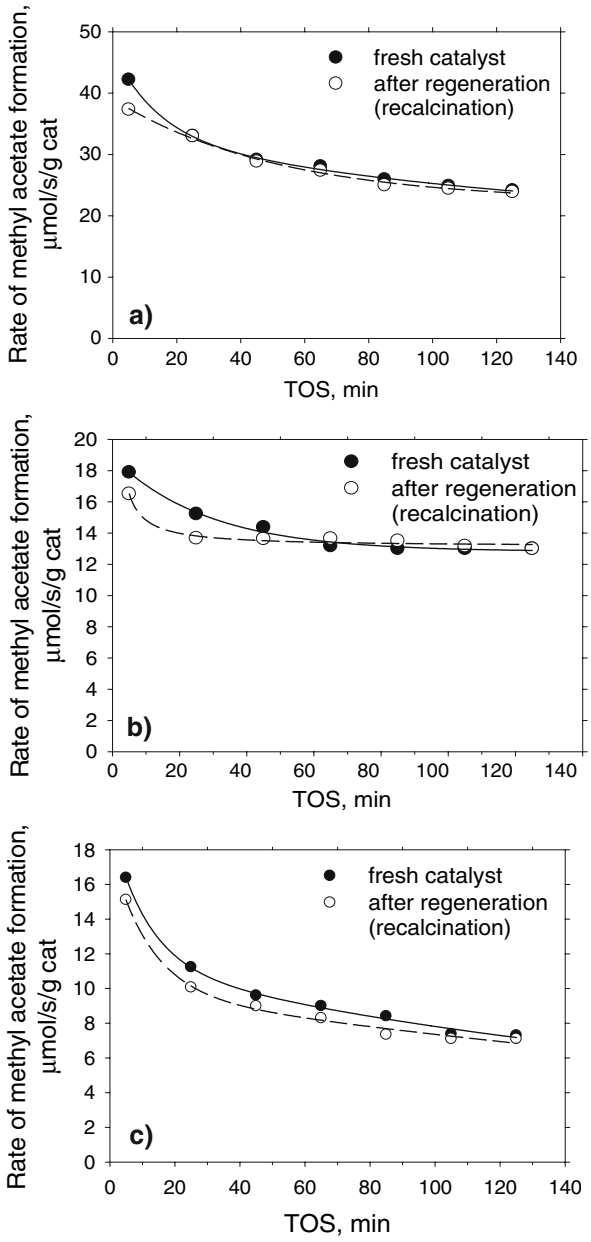

Figure 2. Reusability of inorganic catalysts: (a) Hβ, (b) WZ and, (c) SZ for gas-phase esterification of acetic acid with methanol at reaction temperature 150 °C. (●) fresh catalysts, (○) after re-calcination of the used catalyst at 315 °C for 2 h.

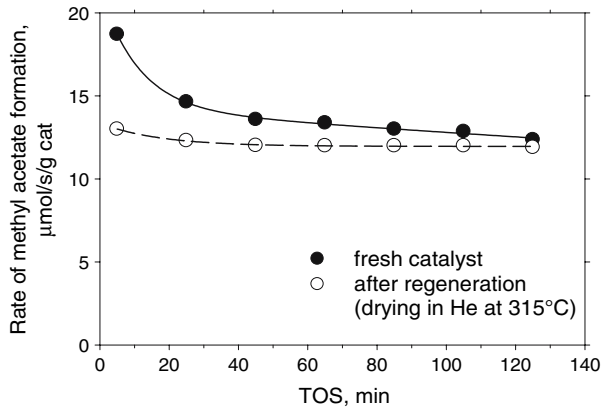

Figure 3. Activity of WZ for gas-phase esterification of acetic acid with methanol at reaction temperature 150 °C: (●) freshly calcined WZ, (○) after dehydration of the spent catalyst in a flow of He at 315 °C for 2 h.

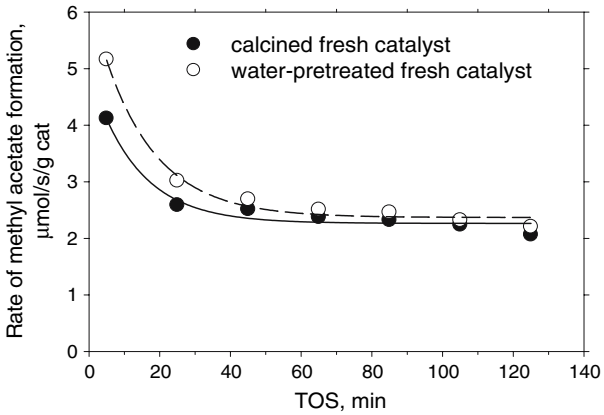

Figure 4. The catalytic activity of gas-phase esterification of acetic acid with methanol over WZ at 130 °C: (●) freshly calcined WZ, (○) water-pretreated freshly calcined WZ.

pyridine (Py) and a sterically hindered 2,6-di-*tert*-butylpyridine (sh-Py) were carried out on WZ. Thus, catalysts were separately pre-saturated with either Py or sh-Py for 120 min at reaction temperature (130 °C). Physisorbed molecules were eliminated under flow of He for 20 min followed by the reaction. The sh-Py is known to strongly adsorb only on Brønsted acid sites; while the Py can interact with both Brønsted and Lewis acid sites [25]. After catalyst poisoning, a 95% reduction on the initial activity was observed for catalyst samples poisoned by both Py and sh-Py, suggesting that Brønsted sites are mainly responsible for the catalysis even though Lewis sites were present in the catalyst, as shown by IR spectra (not shown). However, some residual activity (less than 5%) was observed after poisoning, which could be attributed to weak acid sites adsorbing/desorbing reversibly the Py and sh-Py molecules. Alternatively, the observed residual activity may be due to a small fraction of Brønsted acid sites generated *in situ* by the interaction of the alcohol and the catalyst surface as suggested by Iglesia and co-workers [25]. However, a flow of methanol co-fed with pyridine could not completely suppress the catalytic activity, indicating possibly that alcohol generated Brønsted acid sites may not be the source of the residual activity in this case.

4. Conclusions

The intrinsic activities of zeolite Hβ, SAC-13, SZ, and WZ have been investigated for the gas-phase esterification of acetic acid and methanol. Calculated E_a values for all catalysts were in the range of 55–65 kJ/mol, similar to values for liquid-phase reaction at lower temperatures. On a weight basis, Hβ and SAC-13 showed higher activities than SZ and WZ. Nonetheless, all catalysts exhibited similar catalytic activities on a rate-per-site basis. TOF results suggest that all catalysts have acid sites capable of effectively catalyzing esterification. All the inorganic catalysts used in this study could be almost completely regenerated by re-calcination at 315 °C. For WZ, catalyst deactivation was related to the formation of carbonaceous deposits rather than the accumulation of water on Brønsted acid sites. Selective poisoning experiments for WZ suggested that the reaction primarily took place on Brønsted acid sites.

Acknowledgments

This research was funded by the US Department of Agriculture (Award No 68-3A75-3-147). The authors would like to thank D.E. Lopez for BET surface area analyses and Magnesium Electron (MEL) for providing the WZ and SZ catalysts.

References

[1] E. Lotero, Y.J. Liu, D.E. Lopez, K. Suwannakarn, D.A. Bruce and J.G. Goodwin Jr., Ind. Eng. Chem. Res. 44 (2005) 5353.
[2] X. Chen, Z. Xu and T. Okuhara, Appl. Catal. A 180 (1999) 261.
[3] A. Heidekum, M.A. Harmer and W.F. Hoelderich, J. Catal. 181 (1999) 217.
[4] S.R. Kirumakki, N. Nagaraju and S. Narayanan, Appl. Catal. A 273 (2004) 1.
[5] F. Omota, A.C. Dimian and A. Bliek, Chem. Eng. Sci. 58 (2003) 3175.
[6] H. Matsuhashi, H. Miyazaki, Y. Kawamura, H. Nakamurac and K. Arata, Chem. Mat. 13 (2001) 3038.
[7] S. Ramu, N. Lingaiah, B.L.A.P. Devi, R.B.N. Prasad, I. Suryanarayana and .S.S. Prasad, Appl. Catal. A 276 (2004) 163.
[8] Y. Izumi and K. Urabe, Chem. Lett. (1981) 663.
[9] J.H. Sepulveda, J.C. Yori and C.R. Vera, Appl. Catal. A 288 (2005) 18.
[10] T. Iizuka, S. Fujie, T. Ushikubo, Z.H. Chen and K. Tanabe, Appl. Catal. 28 (1986) 1.
[11] B.R. Jermy and A. Pandurangan, Appl. Catal. A 288 (2005) 25.
[12] I.K. Mbaraka, D.R. Radu, V.S.Y. Lin and B.H. Shanks, J. Catal. 219 (2003) 329.

[13] W.L. Chu, X.G. Yang, X.K. Ye and Y. Wu, Appl. Catal. A 145 (1996) 125.
[14] K.C. Wu and Y.W. Chen, Appl. Catal. A 257 (2004) 33.
[15] E.P. Barrett, L.G. Joyner and P.P. Halenda, J. Am. Chem. Soc. 73 (1951) 373.
[16] Y.J. Liu, E. Lotero and J.G. Goodwin Jr., J. Mol. Catal. A. 245 (2005) 132.
[17] A.M. Camiloti, S.L. Jahn, N.D Velasco, L.F. Moura and D. Cardoso, Appl. Catal. A. 182 (1999) 107.
[18] Y.J. Liu, LoteroE. and J.G. Goodwin Jr, J. Catal. 242 (2006) 278.
[19] S.Y. Kim, J.G. Goodwin Jr., S. Hammache, A. Auroux and D. Galloway, J. Catal. 201 (2001) 1.
[20] K. Shimizu, T.N. Venkatraman and W.G. Song, Appl. Catal. A. 224 (2002) 77.
[21] N.M. Ostrovskii, N.M. Bukhavtsova and V.K. Duplyakin, React. Kinet. Catal. Lett. 53 (1994) 253.
[22] A. Palani and A. Pandurangan, J. Mol. Catal. A. 226 (2005) 129.
[23] J. Bilbao-Elorriaga, J.A. Gonzalez-Marcos, J.R. Gonzalez-Velasco and J.M. Arandes-Esteban, Afinidad, 40 (1983) 459.
[24] L. Li, Y. Yoshinaga and T. Okuhara, Phys. Chem. Chem. Phys. 4 (2002) 6129.
[25] J. Macht, C.D. Baertsch, M. May-Lozano, S.L. Soled, Y. Wang and E. Iglesia, J. Catal. 227 (2004) 479.